CRYOMAGNETICS, INC.
INNOVATIVE TOOLS FOR SCIENTIFIC RESEARCH

Phase I Final Report

Award Number:	DE-SC0019920
Federal Agency:	DOE, Office of Science
Funding Document Number:	20SC502263
Project Title:	Pulsating Heat Pipes for Particle Accelerator Magnet Systems
Principal Investigator:	Adam B. Berryhill
	Director of Engineering
	aberryhill@cryomagnetics.com
	865-813-0647
Submission Date:	January 14th, 2021
DUNS Number:	10-620-3538
Organization:	Cryomagnetics, Inc.
	1006 Alvin Weinberg Drive
	Oak Ridge, TN 37830
Grant Period:	07/01/2019-12/31/2020
Reporting Period End:	1/15/2021
Report Term:	Final

1 Introduction

The primary objective of the Phase 1 award was to investigate the performance of cryogenic pulsating heat pipes (PHPs) and their use in practical large superconducting magnet systems. PHPs exhibit an effective thermal conductivity an order of magnitude and more over high purity metals such as copper and aluminum. They can therefore be utilized to reduce cold mass and effectively transfer heat from the magnet system components such as the coil pack, shields, or current leads to cryocoolers or cryogen reservoirs.

PHPs are comprised of capillary tubing whose internal diameter is sufficiently small so that the surface tension forces of the fluid with which it is charged dominate over gravity forces. The capillary tubing is routed back and forth multiple times between a heat source (evaporator) and a heat sink (condenser), typically closing back upon itself to form a closed loop path for the fluid it contains. An adiabatic region spans the distance between the evaporator and condenser regions. The PHP is charged with a working fluid so that some fraction of the device, called the filling ratio, is occupied by liquid and the remaining fraction by vapor. Upon filling the device, a random distribution of liquid slugs and vapor plugs is formed throughout the internal volume because of the strong surface tension forces. The PHP's remarkable heat transfer properties are operative primarily between the fluid's triple point and critical point and are a result of rapid fluid motions induced by the difference between the higher saturation pressure at the warm end and the lower saturation pressure at the cold end. The 'remarkable' performance is evidenced for example, in the liquid helium regime, where reported values of effective thermal conductivity [2] range as high as 50,000 W/m-K to 150,000 W/m-K. In fact, the heat transfer performance of the PHP is influenced by three groups of parameters: fluid parameters, geometry (or configuration) parameters, and operating parameters.

The thermal conductance of cryogenic PHPs has been shown to depend on their orientation with respect to gravity. PHPs in a fully horizontal orientation exhibit a conductance reduced roughly by a factor of two compared to the same PHP in a fully vertical orientation. Due to the typically complex geometrical arrangement of components in a superconducting magnet system, it is therefore crucial to understand how a PHP extending between a warm and cold region but including both vertical and horizontal path lengths will perform.

The PHP's remarkable heat transfer properties, operative primarily between the fluid's triple point and critical point, limit their useful temperature range to roughly less than 5 K for helium, 14 K to 33 K for hydrogen, 25 K to 44 K for neon, 55 K to 154 K for oxygen, 64 K to 126 K for nitrogen, 84 K to 150 K for argon, and 89 K to 190 K for methane. In many superconducting magnet systems, thermal shields tied to

the intermediate temperatures provided by a cryocooler's upper stage provide the advantage of reducing the heat load impinging on the coldest components of the magnet. For this purpose, superconducting magnet systems can also benefit from the remarkable heat transfer property of a PHP when it is connected between the thermal shield and the upper stage of the cryocooler and filled with a cryogen whose operating range falls in the corresponding temperature range. In the present study a superconducting undulator magnet designed to operate in the 3 K to 4 K range incorporates a thermal shield operating in the 20 K to 30 K range. PHPs utilizing helium and hydrogen are therefore appropriate thermal transport components to investigate for such a superconducting magnet system.

To characterize the dependence of PHP conductance on the relative extent of vertical and horizontal lengths, experiments were designed and carried out that measured the thermal conductance (or thermal resistance) on a set of four PHPs with identical geometries except for their varying aspect ratios (defined below).

2 Accomplishments

A test cryostat for housing the PHP's has been constructed and testing completed at Cryomagnetics. The test cryostat consists of a Cryomech PT410 cryocooler which was used to cool the thermal shield which operates at approximately 45-50K and a second stage platform which operates down to 3K with no external heat load. A platinum resistance thermometer (PT100) of 100 ohms at 273K is used to monitor the shield temperature and a Scientific Instruments ruthenium oxide temperature sensor (RO600) was used to measure the 2nd stage. A Cryomagnetics TM612 read both the PT100 and RO600. The cryostat is designed to be able to test two PHP's at a time to reduce the need for thermal cycling the system. Four pressure sensors (Omega PX119-100AI) were used to monitor the condenser and evaporator pressures for each of the PHPs. A National Instruments CompactDAQ was used to read the pressure sensors and a LabVIEW software program collected the data from all instrumentation. The system cooled down as designed and operates properly. A picture of the test cryostat is shown below.

Figure 1. PHP Test Cryostat

The interior of the cryostat with two of the PHP's installed is shown in the following picture.

Figure 2. PHP Test Cryostat Internal View

3 Products

Four PHPs, two of which are shown above, have been constructed. They consist of 304 stainless steel tubes, whose inner and outer diameters are 0.5 mm and 0.8 mm, respectively. The PHP includes three sections: the evaporator section where heat is applied, the adiabatic section, and the condenser section where heat is extracted by the cryocooler cold head. Both the evaporator section and the condenser section are soldered to separate copper plates, whose sizes are the same: 111.3 mm × 76.2 mm × 3.3 mm. There are four turns at each end of the PHP providing a total of 8 tubes extending between the evaporator and condenser sections. The lengths of the evaporator section and the condenser section are each 111.3 mm, while the length of the adiabatic section is 1000 mm. Two RO600 temperature sensors are used to monitor the temperature at each end of a PHP for redundancy. A 50-ohm cartridge heater is installed on the evaporator end to act as a heat load. A Cryocon Model 24 temperature controller is used to read four

temperature sensors from a single PHP and to control the evaporator heater. A schematic of the system is shown in the figure below.

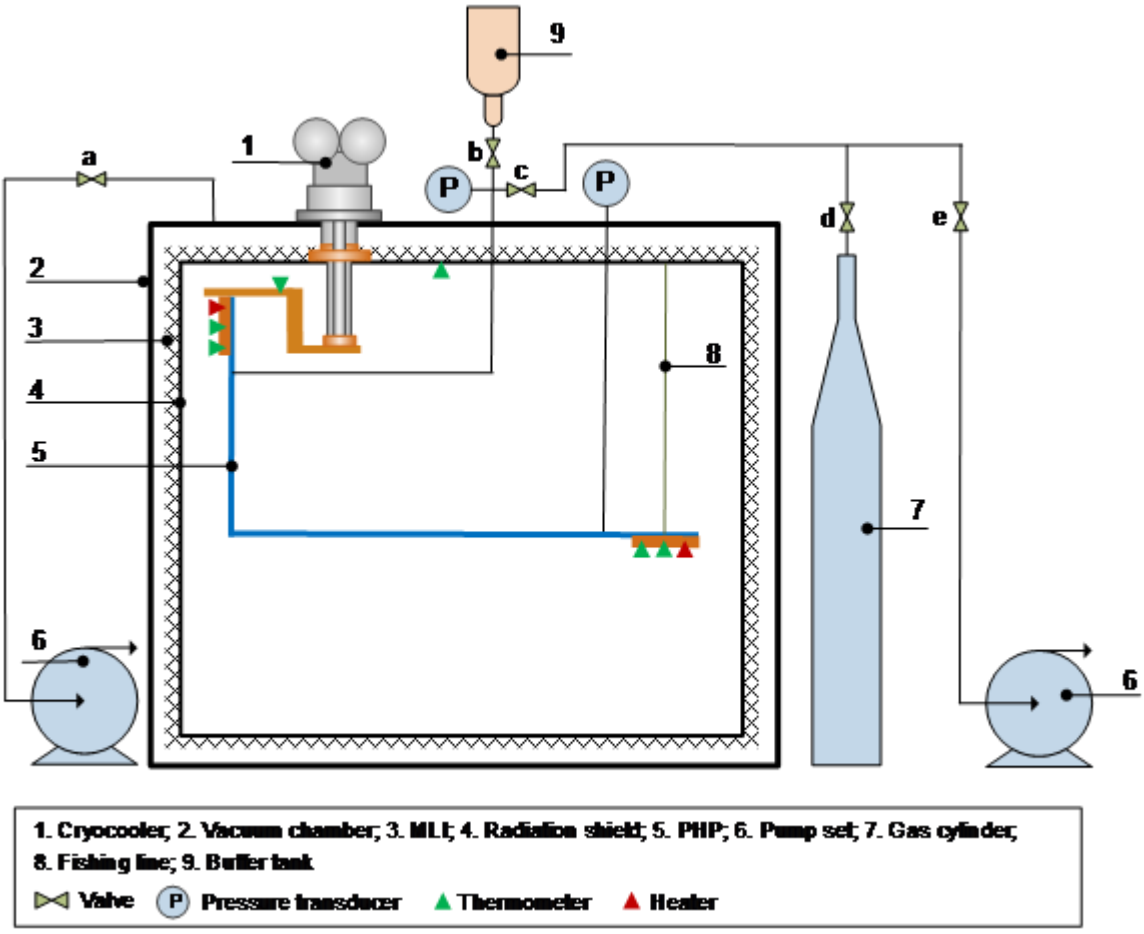

Figure 3. PHP schematic

Before charging the PHP with helium, the buffer tank and the PHP are purged three times to eliminate any residual gas. Then, the valves b, c and d are opened, and the buffer tank and PHP are filled with helium gas to the pressure P_1. Next, valves c and d are closed, and the cryocooler is turned on. Pressure decreases with decreasing temperature. When the pressure is reduced to P_2, valve b is closed. Subsequently, the pressure of the buffer tank remains constant at P_2, while the pressure of the PHP continues to decrease with temperature. Finally, the PHP is allowed to stabilize at a minimum temperature of 2.9 K. The helium in the buffer tank and in the pipe connecting the PHP to room temperature is assumed to behave as an ideal gas, while the gas in the PHP is saturated. The filling ratio (FR) is defined as the ratio of the liquid volume to the total PHP volume, which can be derived from the following mass conservation equation:

$$\frac{P_1(V_{BT}+V_{CP}+V_{PHP})}{R_g T_{amb}}=\frac{P_2 V_{BT}}{R_g T_{amb}}+\frac{P_{sat} V_{CP}}{R_g T_{CP}}+\rho_l(\mathrm{FR}\cdot V_{PHP})+\rho_v(1-\mathrm{FR})V_{PHP} \quad (1)$$

where V_{BT}, V_{CP}, and V_{PHP} are the volumes of the buffer tank, connecting pipe, and PHP, respectively. R_g is the helium ideal gas constant. T_{amb} and T_{CP} are the temperatures of the buffer tank and the connecting pipe, respectively. T_{CP} is calculated as the average of the ambient temperature and the PHP condenser temperature. P_{sat} is the saturation pressure at the filling temperature of 2.9 K, while ρ_l and ρ_v are the densities of saturated liquid and vapor, respectively at that same temperature.

When the filling ratio is 57%@2.9 K, the value of each parameter in Eq. (1) is shown in Table 1.

Table 1 Parameters for obtaining filling ratio

P_1 (kPa)	P_2 (kPa)	P_{sat} (kPa)	V_{BT} (m^3)	V_{CP} (m^3)	V_{PHP} (m^3)
297.2	207.7	20.63	1.11E-03	7.9E-07	1.978E-06
T_{amb} (K)	T_{CP} (K)	ρ_l (kg/m3)	ρ_v (kg/m3)	FR (-)	
300	151.5	142.1	3.9	57%@2.9 K	

The same PHP was tested under different aspect ratios of 1:4, 1:2, 1:1, 2:1 and 4:1 for both helium and hydrogen. At each aspect ratio, the heat load of the evaporator section is gradually increased from zero up to a value close to the cryocooler's maximum cooling capacity. Each heat load is maintained over an extended time (from 15-30 minutes) and then adjusted to allow the PHP to stabilize again at the new heat load. For the helium tests, the filling ratio is set to 56% -57% @ 2.9 K, based on previous research of a helium PHP with a 1000 mm adiabatic section which demonstrated that a filling ratio close to 58% @ 2.9 K is optimal [3]. The measurements obtained with hydrogen used two different filling ratios, 50% and 70%. The data and implications from the helium and hydrogen tests are provided separately and sequentially in the following sections.

3.1 Helium measurements

3.1.1 Cooling the PHP to 4 K

Although the cool down process observed during these measurements is determined by the specific configuration and components used in the test, it is worth noting that the PHP does not provide any thermal advantage to the cool down process. Indeed, due to the stainless-steel capillary used to form this particular PHP, the thermal resistance between the condenser and evaporator ends is very substantial and results in a

significant lag between the temperature decrease of the condenser and that of the evaporator. As mentioned above, a limited number of copper wires were added between the two ends of the PHP to enhance the evaporator cool down. As a result of the modification, both the condenser and evaporator plates cooled to ~ 5 K within 17 hours, while the aluminum thermal radiation shield, due to its larger thermal mass, required an additional 23 hours to reach its final equilibrium temperature of 50 K. By the time that the thermal shield reached its final temperature, the evaporator and condenser plates has also cooled to their coldest temperature near 2.9 K.

Stainless steel has frequently served as the material of choice for PHP construction, primarily to highlight the huge increase in heat transfer between the evaporator and condenser ends when the PHP is charged with the working fluid and operates. However, alternative materials such as copper-nickel would be suitable for constructing the small diameter tubing and would also provide the advantage of a more favorable conductance between the two ends even before the tubing is filled with the working fluid.

It is also of interest to note that in the equilibrated lowest temperature condition, the saturation temperature of the helium vapor and liquid contained inside the PHP, based on the measured pressures were 2.36 K and 2.51 K respectively at the condenser and evaporator ends. In this equilibrated condition, a noticeable temperature difference exists between the copper plates at either end of the PHP and the corresponding fluid temperature inside, presumably from the parasitic heat loads at each end.

3.1.2 Temperature and pressure curves

In keeping with the anticipated dependence on orientation, the helium PHP provided the best thermal performance when the majority of its length was in the vertical orientation. A record of the temperatures and pressures gathered for the 4:1 aspect ratio is shown in Fig. 3. Here, the spatially averaged temperatures for the evaporator and condenser are shown along with the measured pressures in the evaporator and condenser as well as the corresponding saturation temperatures. The heat load applied to the evaporator end is identified at each step in the data. Saturation temperatures are not recorded for any values higher than the critical temperature of helium, 5.2 K, since they are not linked to the measured pressure in the supercritical region. At all heat loads, the difference in pressure between the evaporator and condenser ends is less than 1500 Pa.

In the case of the 4:1 aspect ratio, the maximum temperature measured in the evaporator region approaches 11 K and indicates that the fluid at the evaporator end no longer contains liquid, but rather supercritical, helium. It is significant to note that the helium PHP continues to function under these conditions and is effective at transporting heat. For the smaller aspect ratio configurations comprised of a larger horizontal section the evaporator temperature at the maximum heat load increases, so that with an

aspect ratio of 1:4, the evaporator temperature approaches 28 K while the condenser maintains a temperature below the critical temperature of 5.2 K.

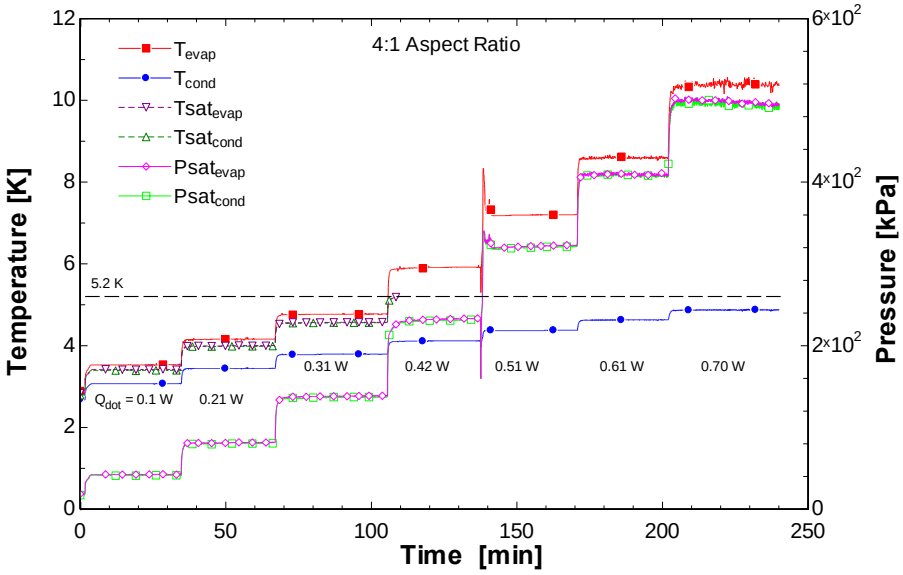

Fig. 3. Temperature and pressure data obtained with the 4:1 aspect ratio helium PHP. The horizontal dashed line identifies helium's critical temperature of 5.2 K.

3.1.3 Thermal resistance and thermal conductivity

The heat transfer characteristic of the helium PHP is best represented in terms of its thermal conductance (in units of W/K) or equivalently its thermal resistance (in units of K/W), as a function of the applied heat load. Fig. 4 displays the thermal resistance of the five helium PHPs measured in this investigation as a function of the applied heat load at the evaporator end.

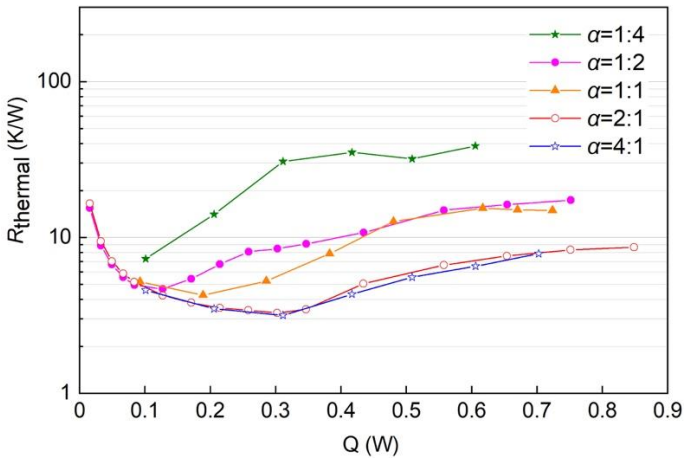

Fig. 4. Thermal resistance data for the helium PHPs

Several important observations can be obtained from the thermal resistance data obtained in the helium PHP:

- The thermal resistance is lowest for the helium PHP with the largest aspect ratio. With α=4 a minimum thermal resistance of 3.2 K/W is measured, and the resistance increases to 7.3 K/W when α=¼. The ratio of these values is like that of fully vertical and fully horizontal helium PHPs.
- The minimum thermal resistance of the helium PHP varies with the applied heat load. Furthermore, the value of the applied heat corresponding to the minimum thermal resistance decreases with the aspect ratio. In the data presented in Fig. 4, the heat load associated with the minimum thermal resistance decreases from 0.3 W to 0.1 W as the aspect ratio decreases from 4 to ¼.
- A summary of the influence of the aspect ratio on the minimum thermal resistance gathered for the helium PHP is shown in Fig. 5 and Fig. 6. Fig. 5 reflects the expected dependence of $R_{thermal}$ on the aspect ratio and one may associate the limiting values of 3 K/W and 7.3 K/W with the asymptotes associated with a fully vertical [4] and fully horizontal helium PHP respectively.

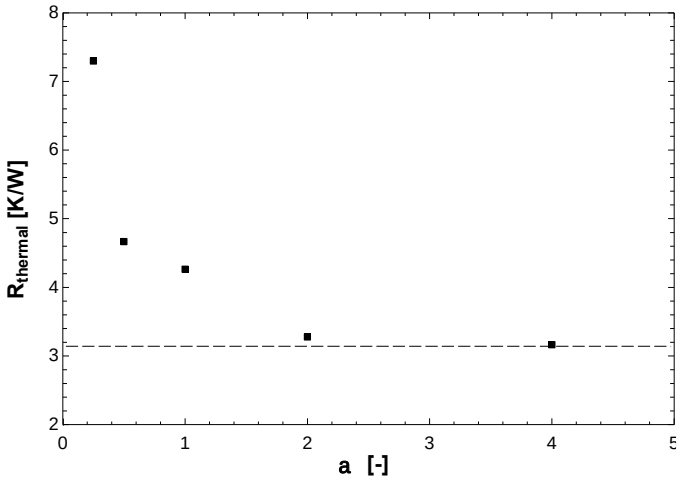

Fig. 5. Minimum thermal resistance vs. aspect ratio (α) for the 8-tube helium PHPs

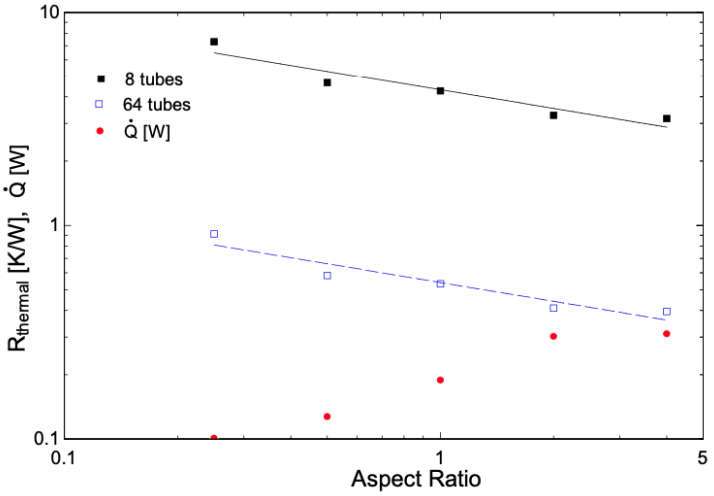

Fig. 6. Minimum thermal resistance values for a single 8-tube and eight parallel 8-tube helium PHP.

- The log-log representation of the minimum thermal resistance data shown in Fig. 6 reveals that within the range of aspect ratios used in the present study, the minimum thermal resistance scales as $c \cdot \alpha^{-0.3}$ where c=4.32 when the PHP is comprised of 8 parallel tubes. The associated heat load for each thermal resistance is also displayed.
- Data from Li, Li, Xu [5] suggest that the thermal conductance (or resistance) of multiple n-turn-PHPs connected in parallel will increase in proportion to the number of n-turn-PHPs connected in parallel and thus scale with the total cross-sectional area of the tubes. The blue dash line displayed in Fig. 6 reflects the expected performance of eight helium PHPs identical to the ones used in this study, connected in parallel between the condenser and evaporator plates. In such a case the combined PHPs would provide 64 tubes in parallel and the thermal resistance would be decreased by a factor of 8 for each of the applied heat load values. With the eight parallel PHP configuration the thermal resistance for the ¼ aspect ratio is 0.91 K/W decreasing to 0.4 K/W for the aspect ratio of 4.

It is of interest also to observe that the minimum thermal resistance of the helium PHP in each configuration occurs at a specific value of the applied heat. That is, there exists an optimal heat load that corresponds to the minimum thermal resistance. In the studies conducted here, the heat load associated with the minimum thermal resistance ranges between 0.1 W and 0.3 W. Optimally designed current leads display a similar feature. That is, their geometry (aspect ratio) is typically designed to correspond to a minimum thermal penalty (W/kA) at the full, steady state, operating current. At current levels greater or less than the

maximum design value, the heat load per current is larger than the optimized value. The PHP should also be designed for optimal operating conditions and will in that case provide a minimum thermal resistance. The data in this study reveals that for heat loads larger or smaller than the optimized value, the thermal resistance increases by up to a factor of 5-6.

Fig. 7 displays thermal resistance information associated with the 8-tube helium PHP having an aspect ratio of 2. If the saturation temperatures generated from the measured pressures in the condenser and evaporator ends reflect the fluid temperatures in those regions, a thermal resistance between the copper plates and the fluid inside the PHP may be obtained. Fig. 7 suggests that much of the thermal resistance between the evaporator and condenser occurs at the solid-fluid interface, and that a much smaller thermal resistance is associated with the temperature difference in the helium between the same two ends. For example, in this case the minimum thermal resistance in the helium is 48 mK/W with a heat load of 0.43 W.

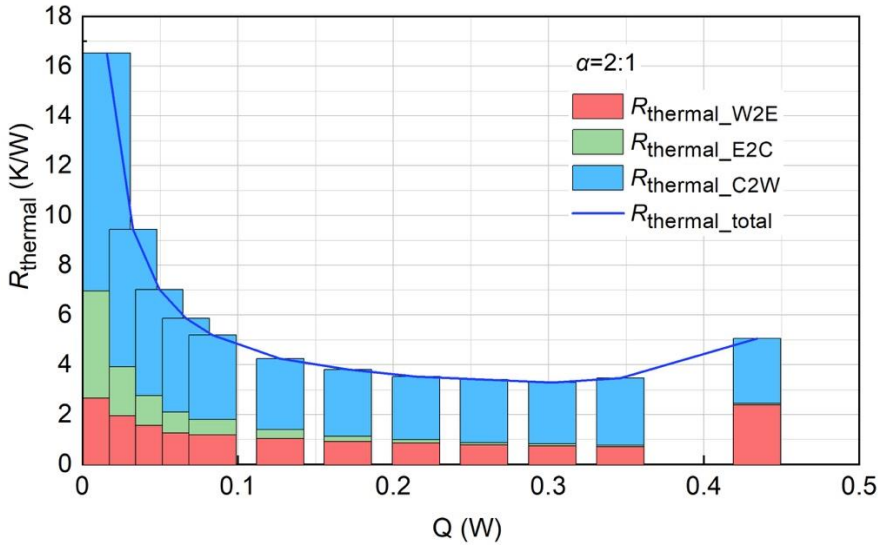

Fig. 7. Thermal resistance contributions. $R_{thermal\_W2E}$ – thermal resistance from the wall to the fluid in the evaporator, $R_{thermal\_E2C}$ – thermal resistance from evaporator fluid to condenser fluid, $R_{thermal\_C2W}$ – thermal resistance from condenser fluid to the wall.

The thermal performance of PHPs is frequently expressed in terms of an effective thermal conductivity (k_{eff}), which is calculated as

$$k_{eff} = \frac{QL_{eff}}{A\Delta T} \tag{2}$$

where Q is the heat load, L_{eff} is the distance between the evaporator midpoint and the condenser midpoint, A is the total cross-sectional area of the fluid in the parallel tubes, and ΔT is the temperature difference between the evaporator and condenser. Fig. 8 displays the effective thermal conductivity values for each of the five PHPs as a function of the applied heat load with the aspect ratio as a variable parameter. Here the maximum effective thermal conductivity values vary from 10 kW/m-K to over 220 kW/m-K. Although these values are amazing in comparison with pure metals such a copper or aluminum, for practical applications such as cooling components in a superconducting magnet, the thermal conductance results shown in Figs. 5 – 7 provide better guidance for design activities.

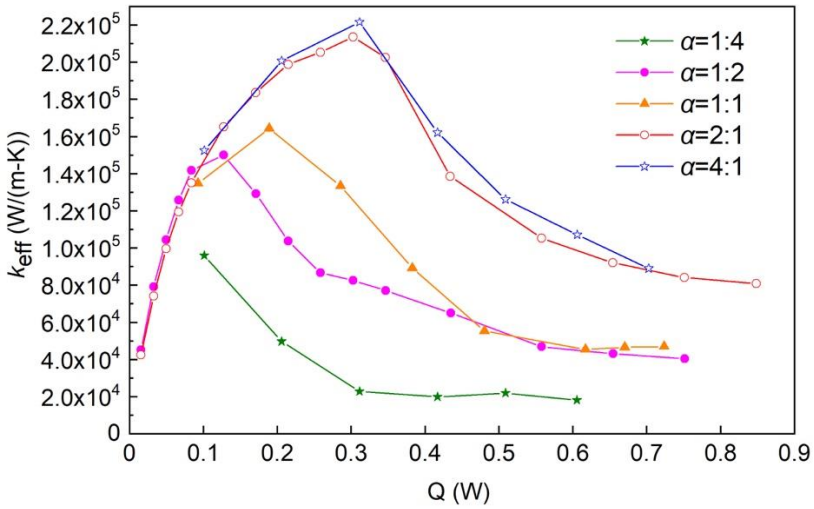

Fig. 8. Effective thermal conductivity for the 8-tube helium PHPs with varying aspect ratio

3.2 Hydrogen measurements

The testing procedure when using hydrogen as the fluid in the PHP was very similar to that when using helium, except that the controlled temperature on the condenser plate was maintained between 19 K and 20 K. Because the cooling capacity of the cryocooler is significantly larger at 20 K (~ 6 watts) than at 4.2 K (1 watt), in the hydrogen tests it was possible to maintain a constant temperature on the condenser plate by reducing the heat applied to the trim heater on the condenser plate as the heat load to the evaporator plate was increased. As with the helium tests, the heat applied at the evaporator plate was increased in a stepwise fashion and held constant for 30-60 minutes to confirm steady-state conditions. In most cases, the test was halted when the evaporator temperatures approached or exceeded hydrogen's critical temperature of 33 K.

The cool-down time to reach 20 K on the PHP and an equilibrium temperature of 59 K on the thermal shield was 18 hours and 36 hours respectively. These times are like those realized during the cool down to 4.2 K because of the relatively minor enthalpy difference of the cold mass between 20 K and 4.2 K.

3.2.1 Data gathered with a 50% fill ratio

A composite graph of the thermal resistance for the hydrogen PHPs with a fill ratio of 50% as a function of the applied heat load with the aspect ratio as a variable parameter is shown in Fig. 9.

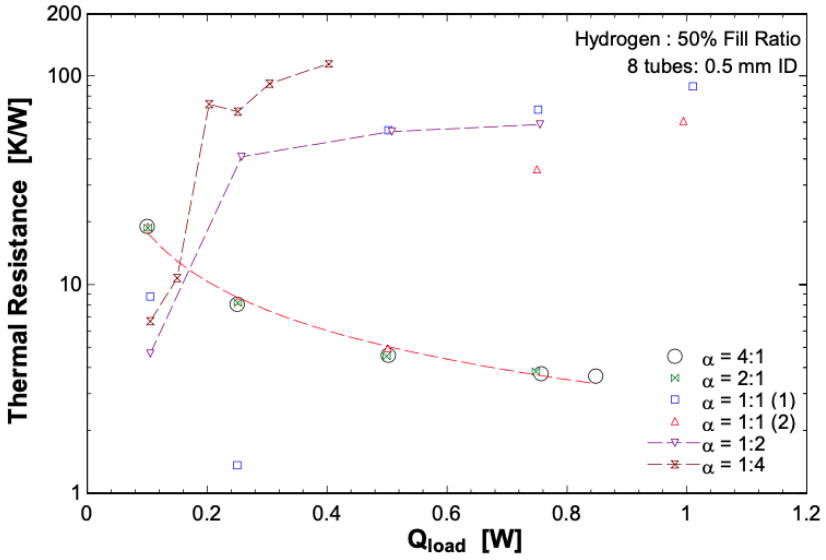

Fig. 9. Thermal resistance of the hydrogen PHP with a 50% fill ratio

Notable features of the data are as follows:

- The larger aspect ratio PHPs display a smoothly decreasing thermal resistance as the heat load is increased, falling to 3.6 K/W at a heat load of 0.8 watts.
- Two different runs with a 1:1 aspect ratio display differing behavior. In the first (1) run, a surprisingly low thermal resistance of 1.4 K/W is realized with a heat load of 0.25 watts, but for larger heat loads, the thermal resistance increases dramatically exceeding 50 K/W. In the second (2) run, the dependence of the thermal resistance follows the same trend as the larger aspect ratio data up to a heat load of 0.5 watts, but also increases dramatically to over 30 K/W as the heat load is increased further. Although the fluid, geometry and initial conditions were all the same, the hydrogen PHP with the 1:1 aspect ratio displays significant variance from run to run.
- The thermal resistance data roughly fall into two separate branches, one associated with the higher aspect ratio configurations displaying smoothly decreasing values of the thermal resistance as the heat load increases, and a second for the configurations with aspect ratios $\leq$

1 in which the thermal resistance trends toward the quiescent fluid limit of 123 K/W. The data suggest that large portions of the horizontal segments toward the evaporator end in the low-aspect-ratio PHPs are vapor locked and produce very little if any fluid motion to effectively transfer heat.

3.2.2 Data gathered with a 70% fill ratio

When the hydrogen PHP is initiated with a 70% fill ratio and subject to the same step wise increase of heat loads to the evaporator, the resulting thermal resistance values are larger than those obtained for the high-aspect-ratio, high-heat-load cases with a 50% fill ratio, but they remain relatively constant over the complete range of heat loads. Furthermore, the thermal resistance values are also relatively insensitive to variations in the aspect ratio. This behavior is displayed in Fig. 10.

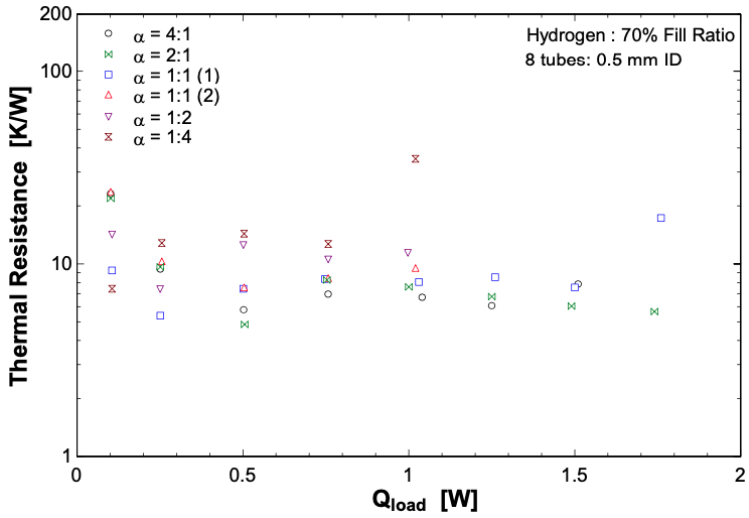

Fig. 10. Thermal resistance of a hydrogen PHP with a 70% fill ratio

One may conjecture that the relatively constant thermal performance with the 70% fill ratio is due to the sustained presence of liquid slugs in the evaporator region for all of the various aspect ratio configurations and applied heat loads. The consistent thermal performance is advantageous for applications in superconducting magnet designs. If a lower thermal resistance than displayed in Fig. 10 is required, multiple PHPs of the same geometry can be used to connect the magnet (or thermal shield) to the cryocooler.

For example, eight such hydrogen PHPs would bring the overall thermal resistance down to or below a thermal resistance of 1 K/W. The crucial design feature would be to ensure a fill ratio of 70%.

As a further point of comparison, measurements of the thermal resistance for the hydrogen PHP with the 1-meter adiabatic length in a fully vertical orientation with the condenser on top and evaporator on the bottom, have been gathered for both the 50% and 70% fill ratios. These values as a function of the applied heat load on the evaporator are shown in Fig. 11. In this data the condenser temperature is held constant at 19 K up to a heat load of 6 watts. For larger heat loads, the condenser temperature also increased with the heat load so that at 9.1 watts the condenser temperature is 25 K while the evaporator temperature is 30.6 K (50% fill ratio) or 30.9 K (70% fill ratio).

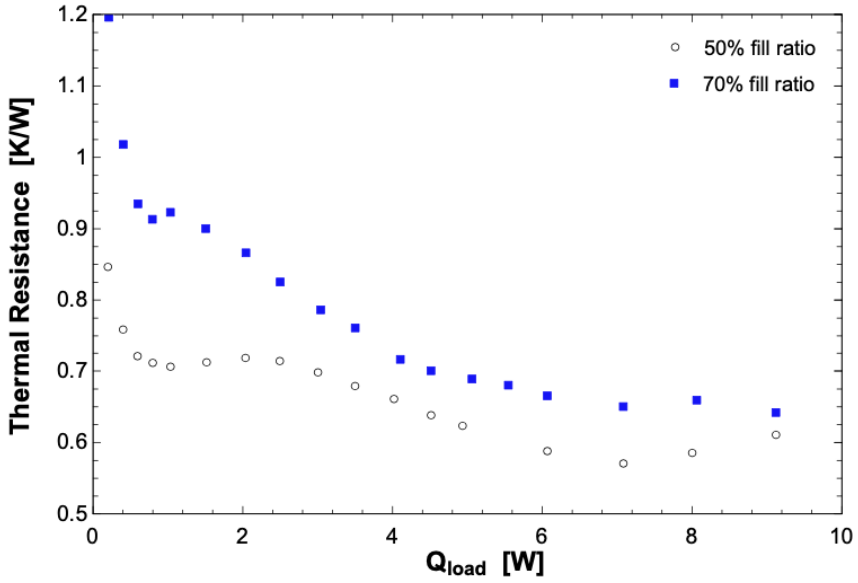

Fig. 11. Thermal resistance of the hydrogen PHP in a fully vertical orientation

4 Conclusions

The experimental activities reported herein characterize the influence of the aspect ratio, that is the ratio of vertical to horizontal lengths, of helium and hydrogen PHPs on their heat transfer performance. The data reveal that the decrease in the overall thermal resistance for the helium PHP as the geometry transitions from vertical to horizontal is in keeping with the published limits of fully vertical and fully horizontal configurations. Moreover, the measured thermal performance of the five different aspect ratios for the 8-tube configuration included in this study reveal that the minimum thermal resistance for helium PHPs varies smoothly as $R_{thermal}=4.32\alpha^{-0.3}$ (K/W) in the range of $0.25 \leq \alpha \leq 4$. Based on the known dependence of overall thermal resistance as a function of the total cross sectional area of the fluid within the parallel tubes one can project that a configuration utilizing eight identical PHPs operating in parallel would result in a

minimum thermal resistance $R_{thermal}=0.54\alpha^{-0.3}$ (K/W) over the same range of α and for the same range of applied heat load, that is from 0 W to 1 W.

The combination of pressure and temperature measurements in this study has enabled a breakdown analysis of the thermal resistance between the evaporator and condenser. The data reveal that the majority of thermal resistance occurs between the copper plate and fluid at each end of the PHP, suggesting that future improvements in materials preparations and fabrication methods could further reduce those thermal resistance contributions.

Results from the hydrogen PHP data reveal that for purposes of consistent thermal resistance values for use in the design of a superconducting magnet system, the PHP should be initiated with a fill ratio of 70%.

In summary, the thermal transport characteristics of the PHP enable a reduction in thermal mass and a large increase in effective thermal conductivity compared to the pure metals typically used for cryogenic thermal bus components such a copper and aluminum. The small size of the capillary tubing however limits the conductance of the PHPs and multiple units configured in parallel are required in order to reduce the associated thermal resistance below 1 K/W. In light of its low mass, passive and large heat transfer capabilities the PHP can provide a valuable component in the overall optimal thermal design for a superconducting magnet system.

5 Demographic Information:

Adam Berryhill:

aberryhill@cryomagnetics.com

Gender: Do not wish to provide

Ethnicity: Do not wish to provide

Race: Do not wish to provide

Disability Status: Do not wish to provide

John Pfotenhauer:

pfot@engr.wisc.edu

Gender: Do not wish to provide

Ethnicity: Do not wish to provide

Race: Do not wish to provide

Disability Status: Do not wish to provide

Xiao Sun:

xsun284@wisc.edu

Gender: Do not wish to provide

Ethnicity: Do not wish to provide

Race: Do not wish to provide

Disability Status: Do not wish to provide

6 Special Reporting Requirements:

None.

References

[1] LD Fonseca, J Pfotenhauer, F Miller, "Results of a three evaporator cryogenic helium pulsating heat pipe," International Journal of Heat and Mass Transfer, 120(2018) 1275-1286.

[2] M Li, L.F. Li, and D Xu, "Effect of number of turns and configurations on the heat transfer performance of helium cryogenic pulsating heat pipe," *Cryogenics* 96 (2018) 159-165.

[3] M Li, L.F. Li, and D Xu, "Effect of Filling Ratio and Orientation on the Performance of a Multiple Turns Helium Pulsating Heat Pipe," *Cryogenics,* vol 100, pp. 62-68 (2019)

[4] T Mito, K Natsume, N Yanagi, H Tamura, T Tamada, K Shikimachi, N Hirano and S Nagaya, "Achievement of High Heat Removal Characteristics of Superconducting Magnets with Built-in Oscillating Heat Pipes," *IEEE Trans. Appl. Supercond.*, vol 21(3), pp. 2470–2473, (2011).